中国激光

飞秒激光成丝过程中的太赫兹波空间强束缚效应

赵佳宇[1]，韩永鹏[1]，朱非凡[1]，郭兰军[2]，张逸竹[3]，彭滟[1]，朱亦鸣[1]，刘伟伟[2*]

[1]上海理工大学太赫兹技术创新研究院，上海 200093；

[2]南开大学现代光学研究所，天津 300350；

[3]天津大学精密仪器与光电子工程学院，天津 300072

摘要 飞秒激光成丝辐射太赫兹波兼具宽频带和高强度特性，其物理机制研究已成为近年来的前沿课题。在此领域，本课题组发现太赫兹波沿激光等离子体光丝被限制在亚波长空间尺度内进行传输，即“太赫兹波空间强束缚效应”，并据此提出了能够全面阐述太赫兹波辐射机理的三过程模型，为统一当前主流宏观与微观理论、化解相关文献中重要结论的矛盾奠定了基础。本文以太赫兹波空间强束缚效应为中心，综述了本课题组近年来的一系列研究工作，包括实验探测技术、物理机理解释及多项创新应用等，并对未来的工作进行了展望。

关键词 物理光学；太赫兹波；飞秒激光成丝；空间束缚；物理机制；超分辨成像

中图分类号 O436 **文献标志码** A **DOI**：10.3788/CJL230778

1 引 言

太赫兹波（THz）频率介于微波与红外之间，太赫兹是新一代信息技术的重要支撑，在生物医学、材料科学等领域具有广阔的应用前景，与太赫兹相关的科技发展将促进人类从全新的视角认识世界[1-6]。太赫兹源是太赫兹技术的核心，近年来涌现出了包括量子级联激光器[7]、光电导天线[8]、光泵浦非线性晶体[9-10]、激光电离固体[11]、激光电离透明介质[12-23]等在内的多个热点方向。

激光电离透明介质技术指飞秒激光在其焦点附近电离透明介质（如空气）形成一段等离子体通道（又称“光丝”）并定向辐射太赫兹波的技术。由于等离子体光丝可以远程产生而且辐射出的太赫兹波具有宽频带和高强度的特征[24-26]，能够克服其在自由空间传输时产生的水汽吸收损耗从而有利于开展遥感与通信等应用[27-28]，因此飞秒激光成丝辐射太赫兹波的物理机制研究成为太赫兹科学的重要分支，而且一直是国际前沿课题。自1993年研究人员首次证实空气等离子体能够辐射太赫兹波[29]至今，以泵浦激光谐波成分命名的“单色场”[30-31]、“双色场”[32-36]和“多色场”[37]系列研究中的里程碑不断出现。以最受关注的双色场为例，国内外学者先后提出了四波混频[32]、瞬态光电流[33]、韧致辐射[38]、离轴相位匹配[39]、光学Cherenkov辐射[40]、线性偶极子阵列[12]等多种物理模型，极大地丰富了领域内的基本理论。

与此同时，主流太赫兹波产生模型尚有争议，重要实验结论仍存在分歧。例如，四波混频[32]和瞬态光电流[33]这两种主流模型就存在根本差异：当太赫兹波产量极大时，前者认为基倍频激光电场的相对相位差为0并给出了实验证据，而后者则推定其为π/2。再如，双色光丝辐射的太赫兹偏振态有椭圆偏振[41-43]和线偏振[44]等不同的实验报道，光电流模型对解释太赫兹脉冲的正交偏振特性仍有困难[45-46]，相比之下，四波混频模型在这方面更具优势[41, 44, 47-48]。此外，在太赫兹波远场发散角对频率的依赖性方面，以“离轴相位匹配模型”[39]为代表的主流观点认为只有大于失相长度（l_d）的双色光丝才能辐射出高频角分布在内、低频角分布在外的太赫兹波。但这既无法解释短光丝的相似辐射行为[49-51]，又与部分文献报道的“高频在外、低频在内”[52]或“角分布与频率无关”[53]的实验结论相悖。

这些亟待解决的矛盾成为双色光丝辐射太赫兹波研究的重大挑战。造成这些矛盾的原因是：飞秒激光成丝是一个复杂的光学现象，具体涉及光克尔自聚焦和等离子体散焦等多个非线性过程[54-55]，单一物理模型很可能无法囊括成丝辐射太赫兹波的全部动力学机制。认识到这一点，本课题组提出了吸纳主流模型在内的多过程理论。

收稿日期：2023-05-04；**修回日期**：2023-05-21；**录用日期**：2023-05-24；**网络首发日期**：2023-06-05

基金项目：国家自然科学基金（12061131010，12074198）、上海市青年科技启明星计划（22QC1400300）

通信作者：*liuweiwei@nankai.edu.cn

2 基于太赫兹波空间强束缚效应的三过程理论

本课题组基于最近实验发现的太赫兹波空间强束缚现象[56]，提出了激光成丝辐射太赫兹波的“三过程模型”[36]，如图 1(a)所示。其中的三条曲线分别代表三种情况下模拟得到的激光焦点处峰值强度沿激光传输方向的演变[35]：Kerr 线代表只考虑 Kerr 效应(突破电离阈值之前)的模拟结果，plasma+dispersion 线代表只考虑等离子体产生与色散的模拟结果，plasma+Kerr+dispersion 线代表上述两个条件都考虑的模拟结果。由此可将激光成丝以突破电离阈值为界，分解为“Kerr 自聚焦”和“plasma 散焦”前后两个过程。在图 1(a-I)所示的第一过程中，由于中性气体分子尚未电离，所以主要考虑泵浦激光及其倍频激光在空气介质中的四波混频效应，此过程会产生太赫兹波。在图 1(a-II)所示的第二过程中，激光光强突破电离阈值后电离空气产生等离子体(自由电子)，等离子体在双色激光脉冲的时间非对称电场的驱动下振荡，形成非零尾电流(又称漂移电流或剩余电流)并辐射太赫兹波。太赫兹波的时间尺度(皮秒)远大于等离子体光丝的建立时间(几十到百飞秒)，同时又远小于等离子体寿命(纳秒)，所以光丝可以看作是太赫兹波的准静态波导。在太赫兹波传输过程中，等离子体自由电子与太赫兹波的相互作用导致太赫兹波被束缚在光丝径向边缘处，此为第三个过程，如图 1(a-III)所示。

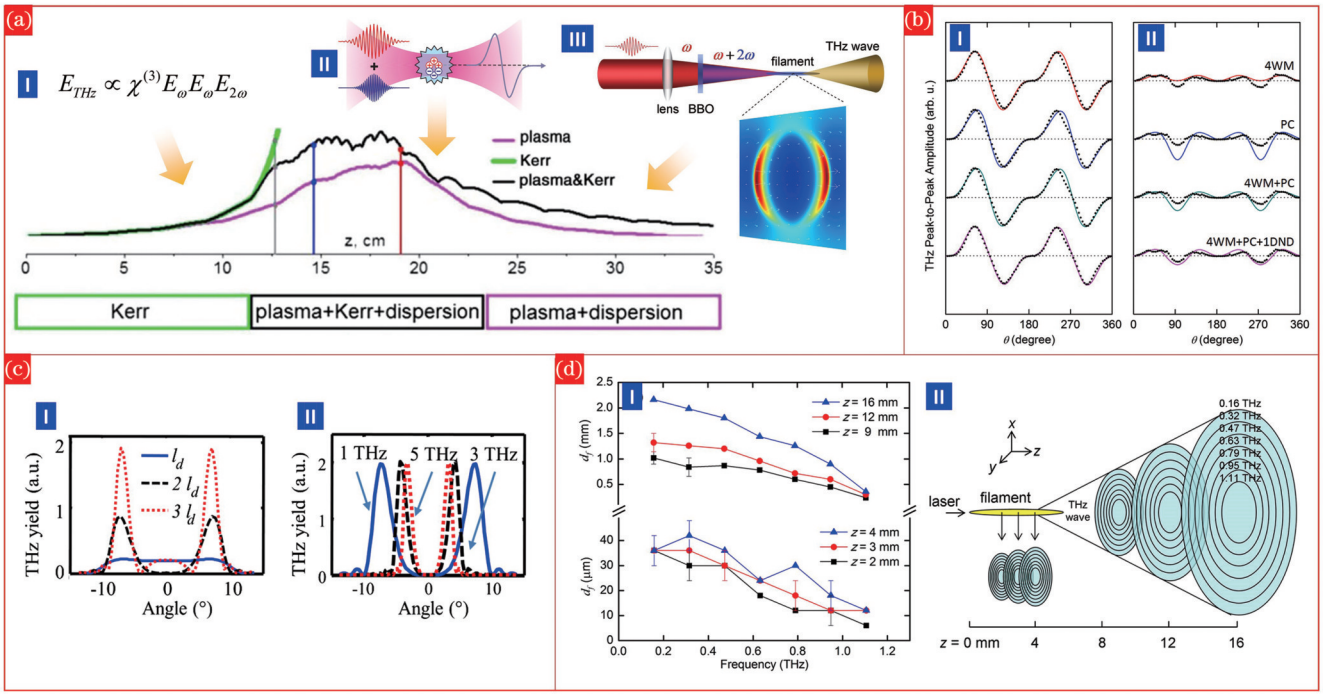

图 1 太赫兹辐射的三过程理论，图片经许可转载自参考文献[24,35-36,39,56]。(a)飞秒激光成丝辐射太赫兹波的三过程模型：(Ⅰ)四波混频和(Ⅱ)光电流振荡分别支配前两个过程[24,35]；(Ⅲ)太赫兹波空间强束缚传输作为第三过程[56]。(b)三过程模型获得了最佳的拟合效果[36]，其中黑点是实验探测的正交太赫兹偏振分量的时域峰峰值随倍频晶体转角的演变，拟合线分别是使用四波混频(4WM)、光电流(PC)、4WM+PC 和三过程模型(4WM+PC+1DND)的拟合结果。(c)离轴相位匹配模型计算得到的不同光丝长度下太赫兹波的远场辐射包络(Ⅰ)与频率依赖关系(Ⅱ)[39]。(d)太赫兹波空间强束缚情况下光丝区域和远场的太赫兹光束直径变化及其频率依赖性(Ⅰ)与对应的示意图(Ⅱ)[56]

Fig. 1 Three-process theory of terahertz (THz) radiation, with figures reproduced with permission from Ref. [24, 35-36, 39, 56]. (a) Three-process model of THz wave generation via femtosecond laser filamentation: (Ⅰ) four-wave mixing (4WM) and (Ⅱ) photocurrent (PC) oscillation dominate the first two processes[24,35], respectively; (Ⅲ) the spatially confined transmission of THz waves is considered as the third process[56]. (b) Best fittings of the experimental results are achieved with the three-process model[36]. Black dots represent the experimental evolution of the time-domain THz peak-to-peak amplitudes in orthogonal directions with the rotation angle of the frequency-doubling crystal. Fitting lines correspond to the results obtained by using 4WM, PC, 4WM+PC and the three-process model (4WM+PC+1DND), respectively. (c) Far-field radiation profiles (Ⅰ) and the frequency dependence (Ⅱ) of THz waves from different filament lengths are obtained via the off-axis phase-matching model[39]. (d) Diameter variation and frequency dependence of THz beams in the filament region (with strong spatial confinement) and far field[56] are shown in (Ⅰ) as experimental results, and in (Ⅱ) as a schematic view

基于上述分析，采用四波混频、光电流这两个主流模型以及本课题组提出的一维负介电常数波导模型对三个过程的太赫兹辐射与传输行为进行解释。可以注意到，若只考虑第一或第二过程，即采用两个主流模型

单独进行预测，则预测得到的太赫兹波正交偏振分量都不能令人满意[如图 1(b)中的红线、蓝线所示]，而且两个模型的预测结果存在较大差异。鉴于此，本课题组独辟蹊径，提出了用两个过程偏振分量的叠加结果来研究光丝辐射太赫兹脉冲物理机制的新思路，即根据两种主流模型预测的偏振分量的振幅比例来推导两种辐射机制各自的贡献。可以看出，本课题组所提模型综合考虑了四波混频和光电流模型的共同作用，对太赫兹偏振分量数据随倍频晶体转动规律的拟合更加准确，如图 1(b)中的绿线所示。最后，本课题组将“太赫兹波空间强束缚效应”作为不容忽视的“第三过程”考虑进来。由于太赫兹波被限制在一个直径约为波长几十分之一的空间尺度内进行无衍射传输[如图 1(a-III)所示]，光丝成为太赫兹波段的亚波长“负介电常数波导”，这时就需要考虑太赫兹波与等离子体相互作用后的空间模式分布、能量损耗以及频谱变化等。最终结果如图 1(b)中的粉线所示，获得了对实验结果的最佳拟合。

另外，对于上文提到的太赫兹辐射远场角色散的高低频分布争议，也应将太赫兹波沿着光丝存在束缚传输效应考虑进来，因为其传输模式的演变将给远场太赫兹辐射与空间角分布带来多样性[57]，这种多样性是解释文献中不同实验现象的可行途径，有潜力化解角色散变化趋势的矛盾。如，离轴相位匹配模型在长光丝($l>l_d$)情况下可以模拟得到显著的太赫兹远场环状辐射[如图 1(c-I)所示]与高频在内低频在外的角色散分布[如图 1(c-II)所示]，但在短光丝($l\approx l_d$)情况下无法模拟复现以上辐射特征[如图 1(c-I)中的蓝线所示]。对此，本课题组通过实验和负介电常数波导模型证实了短光丝同样可以产生此类频率依赖的远场辐射行为[56]，这是太赫兹光束从光丝内束缚态过渡到光丝后衍射态的一个固有趋势，如图 1(d-I)、图 1(d-II)所示。

综上，本课题组提出的“四波混频＋光电流＋负介电常数波导模型”三过程新机理，克服了单一物理模型的局限与不足、架通了主流模型之间的关联、统一了长期无法兼容的基本理论，从而得以全面合理地解释双色场辐射太赫兹偏振态随倍频晶体转动的演变过程[如图 1(b)所示]以及近场太赫兹模式和远场太赫兹空间啁啾等实验结果，为化解太赫兹辐射角分布等实验结论的矛盾提供了新思路。接下来本文将从实验、原理和应用三方面梳理本课题组在太赫兹波空间强束缚效应方面开展的一系列研究工作。

3 太赫兹波空间强束缚现象的实验探测技术

对太赫兹波空间强束缚现象进行实验探测需要首先突破“激光烧蚀”这个难题，因为等离子体区域的光强很高，给近场探测束缚其中的太赫兹波带来了巨大挑战。在这一方面，本课题组创新地采用耐激光烧蚀的非极性材料(如薄陶瓷片等)截断光丝，这样就可以有效避免后续光学元件被光丝损伤；同时，非极性材料又可以使太赫兹波较好地透过，便于太赫兹波电场的探测。基于此，本课题组先后提出了“纵向截丝”、“横向截丝”和“二维扫描成像”等三种太赫兹波近场诊断新手段，并分别对等离子体光丝区域的太赫兹折射率、太赫兹光束直径和太赫兹模式分布进行了探测，充分验证了太赫兹波的空间强束缚效应。

3.1 纵向截丝法

纵向截丝法是利用非极性板材截断光丝(阻断光丝在其后形成)并将板材沿光丝纵向平移的过程，截丝板材如薄陶瓷片[58-59]等既能够抵御光丝烧蚀又能使太赫兹波透射(约为 50%)。在板材纵向平移过程中，光丝长度逐渐增大[如图 2(a-I)所示]，同步探测到的太赫兹脉冲振幅最大值发生了明显的时域前移[前移了约 0.3 ps，如图 2(b-I)所示]。这种独特的太赫兹相速度超光速现象可由太赫兹波沿等离子体光丝进行导引传输来解释。由图 2(b-I)所示的太赫兹时域信息可推知频域的相位分布；之后根据相位随传输距离的变化计算太赫兹折射率，如图 2(b-II)中黑色圆圈所示，可以看到太赫兹折射率皆小于空气折射率，说明太赫兹波并没有在空气中进行衍射传输；对等离子体中的太赫兹折射率进行理论计算后发现等离子体密度 N_e 为 1×10^{14} cm^{-3} 时可以实现对实验结果的较好拟合[如图 2(b-II)中的实线所示][60]，从而证明了太赫兹波在等离子体中传输。此外，拟合使用的 N_e 值小于光丝轴上的 N_e 值(约为 $10^{16}\sim10^{17}$ cm^{-3})，这预示着太赫兹传输模场强度集中在光丝的径向边缘处。关于这一点，将在第 4 部分进行更详细的分析。

3.2 横向截丝法

还可以采用横向刀片法(KE 法)截丝获取太赫兹光束的直径信息从而探测太赫兹波的空间强束缚效应[61]，如使用电木板作为 x 向截丝材料，如图 2(a-II)所示。与陶瓷片相比，电木板同样可以抵御强激光烧蚀，但太赫兹波的透过率很低(约为 4%)，所以能够同时切断光丝和太赫兹光束，达到刀片法测量直径的目的。一个典型的探测结果如图 2(c-I)所示，太赫兹光束直径约为 $d=20$ μm。将 d 随 z 变化的完整数据绘制于图 2(c-II)中，可见：在光丝区域内，太赫兹光束直径由 20 μm 缓慢增加到 50 μm，并在光丝后迅速陡增至 1～6 mm。所以，太赫兹光束在光丝区域被限制在一个直径远小于其波长的空间尺度内，这就证实了太赫兹波沿等离子体光丝的强束缚传输。

3.3 二维扫描成像

对太赫兹波空间强束缚现象最直接的探测方法是对等离子体内部的太赫兹模场分布进行显微成像[58]，如图 2(a-III)所示，同样使用陶瓷片截断光丝，并在其后表面紧附一个金属微孔(直径约为 10 μm)，并将二

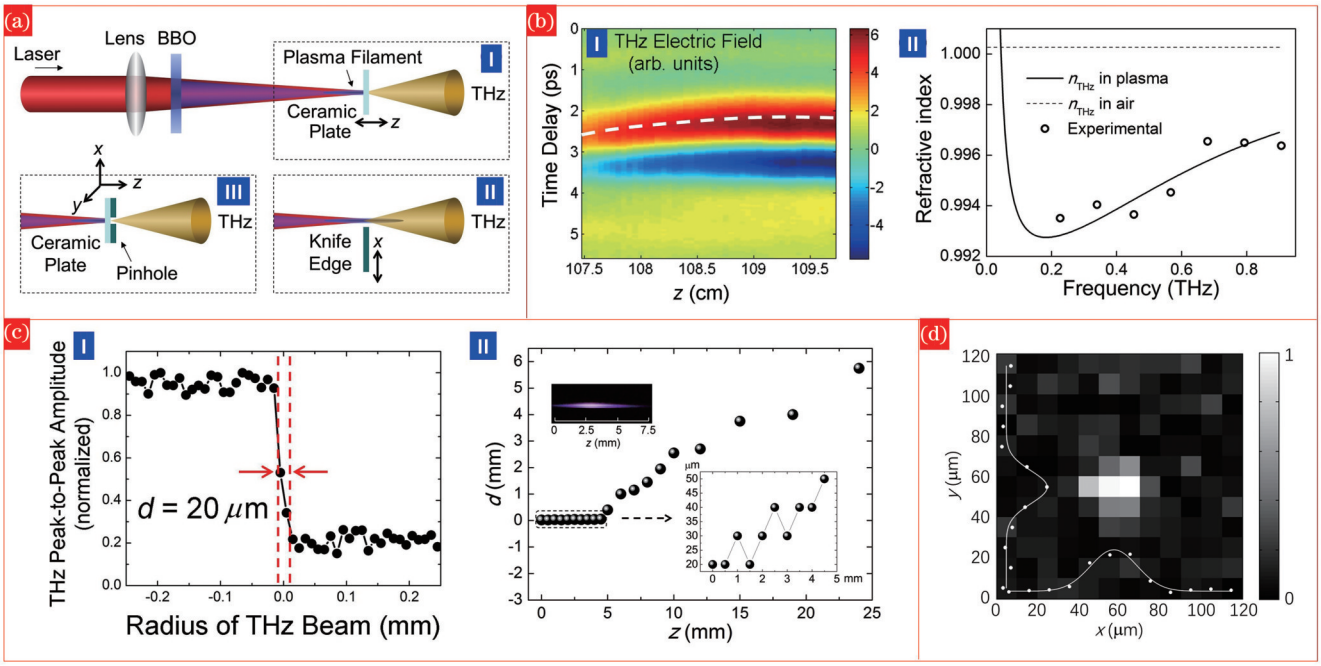

图 2 太赫兹波空间强束缚现象的实验探测，图片经许可转载自参考文献[58-60]。(a)太赫兹波空间强束缚现象的三种实验探测手段[58]，即纵向截丝(Ⅰ)、横向截丝(Ⅱ)和二维扫描成像(Ⅲ)；(b)纵向截丝探测到的太赫兹脉冲时域前移现象(Ⅰ)[59]以及由此计算得到的太赫兹折射率分布(Ⅱ)[60]；(c)横向刀片法截丝测量的一组典型数据(Ⅰ)以及太赫兹光束直径随光丝传输距离的演变(Ⅱ)[61]，其中(Ⅱ)图左上角所示插图是光丝的侧向照片；(d)光丝横截面内太赫兹分布的二维扫描成像结果[58]

Fig. 2 Experimental detection skills of strong spatial confinement phenomena of THz waves, with figures reproduced with permission from Ref. [58-60]. (a) Three experimental methods for detecting the strong spatial confinement of THz waves[58] are longitudinal translation of the blocker (Ⅰ), knife-edge (KE) measurement (Ⅱ), and two-dimensional scanning imaging (Ⅲ); (b) the temporal advance phenomenon of THz pulses (I)[59] given by the longitudinal method, which further leads to the THz refractive index distribution as shown in (Ⅱ)[60]; (c) a typical result given by the transverse KE detection method (Ⅰ) and the evolution of THz beam diameters with the filament propagation distance (Ⅱ)[61], where the side view of the filament can be found in the upper left corner of (Ⅱ); (d) the two-dimensional scanning imaging result of THz distributions within the cross section of the filament[58]

者一起在x-y平面内移动，实现对光丝横截面内太赫兹分布的二维扫描。成像结果如图 2(d)所示，太赫兹光束的x、y向半峰全宽分别约为 27 μm 和 20 μm，与图 2(c)所示刀片法探测结果基本一致，进一步证明了太赫兹波被束缚在光丝中传输。值得说明的是，这里的成像结果并未像图 3 模拟的那样呈现中空环状分布，这是因为金属微孔直径受限于成像信噪比无法足够小，所以成像分辨率不足；此外，扫描成像使用的 Golay cell 探测器的带宽为 0.1～30 THz，无法准确体现图 3 所示模拟的单频、低频(0.1～1 THz)太赫兹模场分布效果。

4 太赫兹波空间强束缚效应的机理解释

本课题组分别采用数值模型和解析模型对光丝区域的太赫兹传输模式进行了推演，并将两种方法得到的结果进行了印证，结果表明光丝作为亚波长尺度的太赫兹波导能够将 0.1～1 THz 范围内的太赫兹能量束缚在其径向边缘处，形成独特的空芯环状电场分布。太赫兹波空间强束缚效应的机理解释既补充了现有成丝辐射太赫兹波的基本理论，也为本课题组提出的“三过程模型”奠定了重要基础。

4.1 数值模型

本课题组首先采用 Comsol 软件构建了等离子体光丝的径向介电常数分布数值模型，其中光丝径向 N_e 分布和太赫兹折射率分布如图 3(a-I)中的蓝线和红线所示，后者在 r=55 μm 附近存在极小值；然后使用全向量有限元法(FEM)对太赫兹本征模式(0.2～0.6 THz)进行了数值模拟[61-63]，结果如图 3(a-II)所示，可以看出太赫兹模场分布在以光丝为中心的亚波长宽度的环状区域内，且模场最大值位于折射率谷值处，如图 3(a-I)中的黑线所示。此外，本课题组还在更宽的频率范围内(0.1～10 THz)进行了模拟[57]，有效揭示了太赫兹模场随着频率增大从光丝径向边缘(低频)逐渐向光丝中心演变(高频)的全过程。需要说明的是，以上数值模拟采用的等离子体密度和光丝直径等参数都是光丝焦点处的数值，所以模拟得到的太赫兹模场直径[约为 100 μm，如图 3(a-II)所示]会比实验数值[如图 2(c)～(d)所示]稍大。

4.2 解析模型

上述数值模拟得到的太赫兹模场分布特征同样可

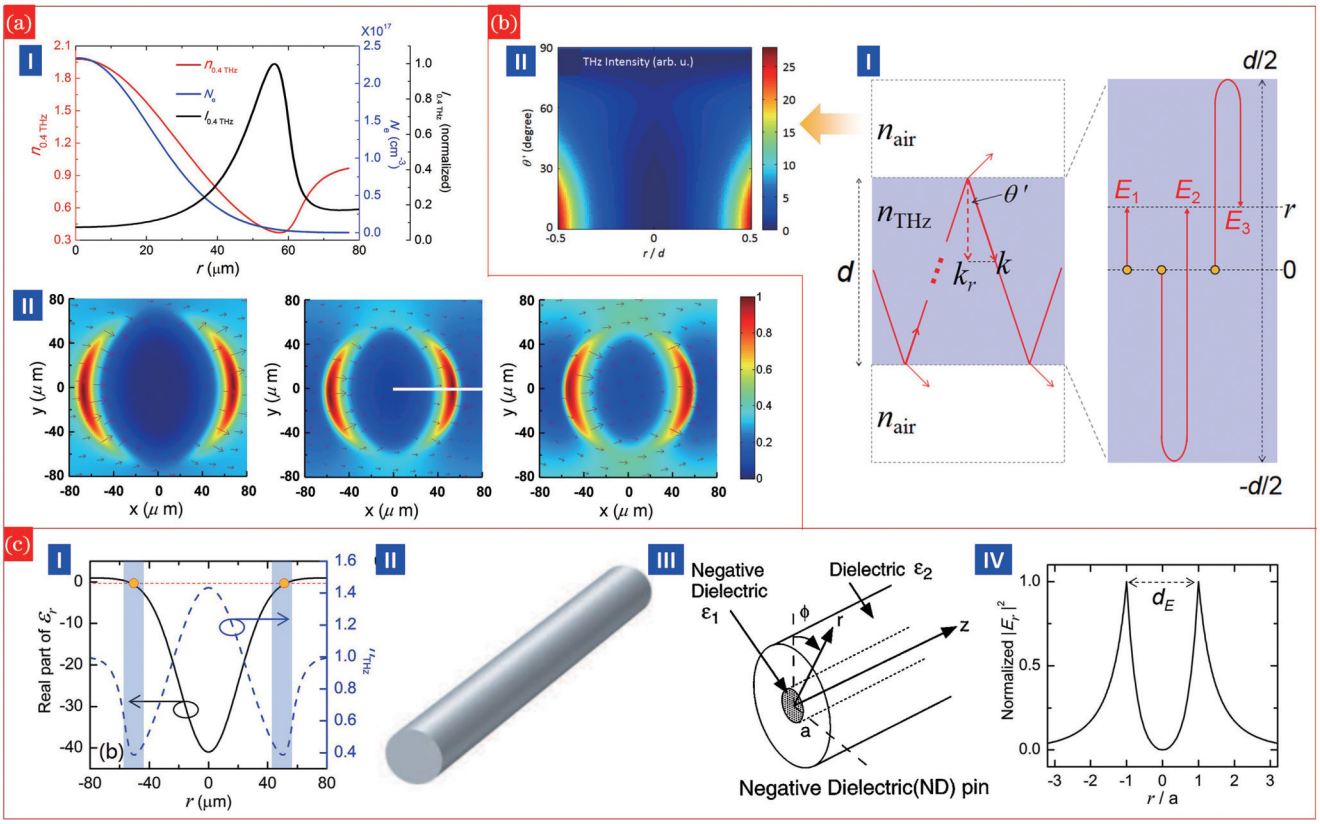

图 3 太赫兹波空间强束缚效应的理论模型，图片经许可转载自参考文献[56-57，61-62]。(a)数值模型[61]：(Ⅰ)等离子体密度、0.4 THz折射率和模拟得到的太赫兹模场的径向分布；(Ⅱ)0.2、0.4、0.6 THz的模场截面图。(b)微腔振荡模型[57]：(Ⅰ)太赫兹波在“空气-等离子体-空气”简化腔内振荡的光线追迹图；(Ⅱ)腔内太赫兹模场分布图。(c)一维负介电常数波导(1DND)模型[56,62]：(Ⅰ)等离子体光丝的径向介电常数实部(黑色实线)和折射率分布(蓝色虚线)[56]；(Ⅱ)(Ⅲ)金属纳米细丝作为负介电常数光波导的示意图[62]；(Ⅳ)1DND模型给出的太赫兹模场径向分布，其中a定义为$\mathrm{Re}[\varepsilon_r]=0$时的径向距离[56]

Fig. 3 Theoretical models for the spatial confinement effect of THz waves, with figures reproduced with permission from Ref. [56-57, 61-62]. (a) Numerical model[61]: (Ⅰ) the plasma density, refractive index at 0.4 THz and radial distribution of the simulated THz modal field; (Ⅱ) the cross sections of THz modes at 0.2, 0.4 and 0.6 THz. (b) Micro-cavity oscillation model[57]: (Ⅰ) the ray-tracing diagram of THz wave oscillations in a simplified “air-plasma-air” cavity; (Ⅱ) the field distribution of the THz mode inside the cavity. (c) One-dimensional negative dielectric (1DND) waveguide model[56,62]: (Ⅰ) the radial real part of the dielectric constant (black solid line) and refractive index distribution (blue dashed line) of the plasma filament[56]; (Ⅱ)(Ⅲ) the schematic diagram of a metal nanowire as a negative dielectric constant optical waveguide[62]; (Ⅳ) the radial distribution of the THz modal field given by the 1DND model, where “a” is defined as the radial distance at which $\mathrm{Re}[\varepsilon_r]=0$[56]

以采用解析模型获得，这里介绍两项本课题组的工作，分别是微腔模型和一维负介电常数波导(1DND)模型。前者将光丝区域的太赫兹折射率分布简化为一个具有“空气-等离子体-空气”三层结构的谐振微腔[57]，如图3(b-Ⅰ)所示，然后追迹太赫兹光线在其中的振荡叠加过程，由此解析计算等离子体区域内任意径向位置处的太赫兹模场强度。计算结果如图3(b-Ⅱ)所示，可见，太赫兹强度极大值出现在径向边缘处，即太赫兹波空间束缚现象，这与上节所述的数值模拟结果基本一致。

相比于微腔模型，1DND模型[56]更加完备。简要来说，本课题组通过计算光丝径向的相对介电常数实部$\mathrm{Re}[\varepsilon_r]$分布[如图3(c-Ⅰ)中的黑色实线所示]，发现光丝具有负介电常数金属波导的特征，如图3(c-Ⅱ)和图3(c-Ⅲ)所示。接着，在柱坐标系下求解麦克斯韦方程组[62,64]，得出传导模式在负介电常数纤芯和空气包层中的解析解。最后计算得到的等离子体光丝区域0.4 THz模场强度$|\boldsymbol{E}_r|^2$如图3(c-Ⅳ)所示，可见模场强度$|\boldsymbol{E}_r|^2$呈离轴环状分布。所以，基于1DND模型解析求解得到的太赫兹模场分布特点与数值模拟结果一致。不仅如此，两种模型给出的太赫兹模场径向极大值的位置相同。一方面，数值模型极大值位于折射率谷值处，这一点在图3(a-Ⅰ)中有过描述；另一方面，解析模型极大值出现在正、负介电常数交界处，即$\mathrm{Re}[\varepsilon_r]=0$处，如图3(c-Ⅳ)所示。综合以上两点，从图3(c-Ⅰ)所示的淡蓝色阴影区域可以看出二者其实是重合的。

5 太赫兹波空间强束缚效应的应用

太赫兹源在真正走向成熟之前，仍面临诸多瓶颈和挑战，如：1)由于衍射极限的限制，太赫兹成像受限于其亚毫米波长，成像分辨率为毫米量级，这是太赫兹

成像技术应用面临的基础性难题之一，而显著提升分辨率的手段如近场探针扫描显微术会极大地降低太赫兹能量利用率和成像信噪比；2）太赫兹波与物质的非线性相互作用往往需要强太赫兹电场强度和极端泵浦激光能量，从而极大地限制了非线性太赫兹光源的普及和使用；3）宽带太赫兹偏振调控对于太赫兹通信、生物医药检测等领域意义重大[13]，光丝作为代表性的宽带太赫兹源，其输出太赫兹偏振态的调控方式需要进一步拓展。针对上述难题，本课题组基于太赫兹波空间强束缚效应开展了一系列研究工作，分别实现了能量无损的太赫兹超分辨成像、低泵浦功率下的强太赫兹电场以及宽带太赫兹单脉冲偏振态的灵活调控。

5.1 能量无损的近场扫描太赫兹超分辨成像

束缚在光丝中的太赫兹光束突破了衍射极限，直径远小于其波长，可直接用作扫描成像的太赫兹源，实现亚波长成像分辨率[61]（无须使用探针或小孔等辅助手段），所以太赫兹能量可全部用于成像而无损失。实验装置如图 4（a-I）所示，待成像样品是含有多个通孔（直径约为 600 μm）的电木板，与其密接的陶瓷片用于阻断光丝对样品的烧蚀，从通孔透射的太赫兹能量最终被探测。图 4（a-II）分别给出了光学成像（分辨率约为 5 μm）和太赫兹扫描成像结果。对比光学成像和太赫兹扫描成像结果可见，后者的每个孔都清晰可见，而且孔的边缘都非常清晰。进一步沿绿色点线提取一列通孔的成像包络分布并将其绘制于图 4（a-III）中，可见太赫兹成像（蓝色方块）的孔边界与光学成像一样清晰。值得一提的是，实验中太赫兹脉冲的峰值波长是 750 μm，这个数值本身比通孔直径还要大，因此这种太赫兹成像方法具有亚波长尺度的超分辨能力。此外，由于被空间束缚和集中的太赫兹能量全部用于成像，所以此成像技术在取得高分辨率的同时也保持着良好的成像对比度。

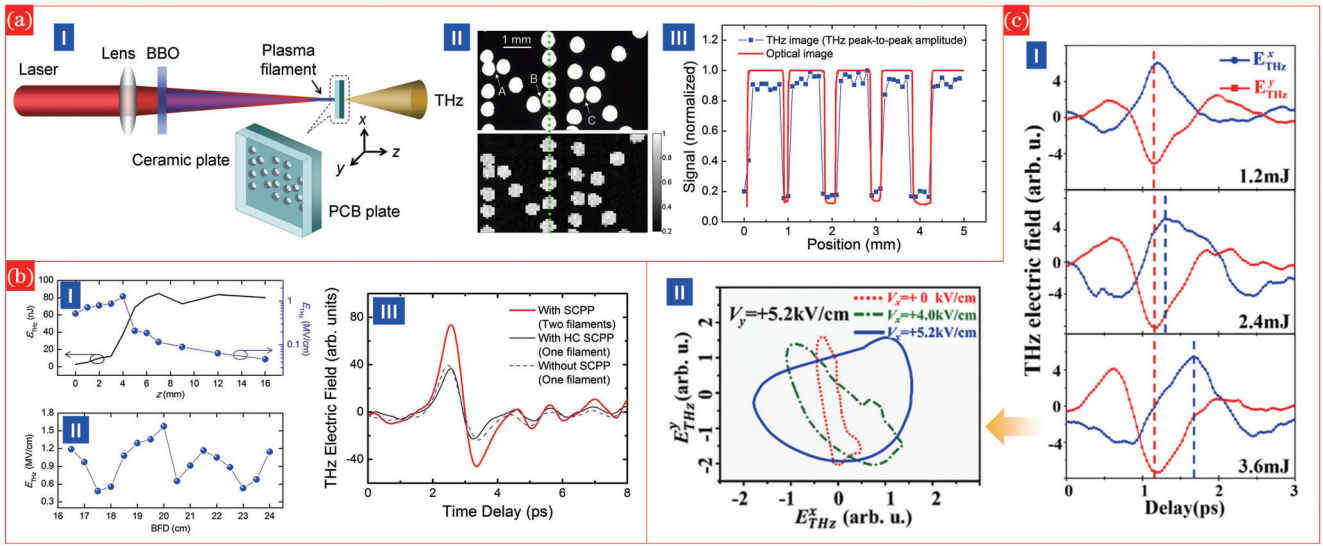

图 4 太赫兹波空间强束缚效应的应用，图片经许可转载自参考文献[56，61，65-68]。（a）超分辨太赫兹成像[61]：（Ⅰ）实验装置示意图；（Ⅱ）光学成像与太赫兹成像的对比；（Ⅲ）一维数据对比。（b）太赫兹能量与电场强度沿光丝的演变（Ⅰ）[56]、太赫兹电场最大值随倍频晶体 BBO 到焦点距离（BFD）的变化（Ⅱ）[56]以及双丝辐射太赫兹波的增强（Ⅲ）[65]。（c）通过改变泵浦激光功率和光丝的横向静电偏压来调控太赫兹波正交分量的相对时间延迟（Ⅰ），从而实现太赫兹输出偏振态的转换（Ⅱ）[66-68]

Fig. 4 Applications based on the strong spatial confinement of THz waves, with figures reproduced with permission from Ref. [56, 61, 65-68]. (a) Super-resolution THz imaging[61]: (Ⅰ) the experimental setup; (Ⅱ) comparison between the optical and THz images; (Ⅲ) comparison of one-dimensional data. (b) Evolution of THz energy and electric field intensity along the filament (Ⅰ)[56], the relationship between the maximum THz electric field and the distance from the BBO crystal to the focal point (BFD) (Ⅱ)[56], and the enhancement of THz radiation with a dual-filament array (Ⅲ)[65]. (c) By adjusting the pumping laser power and the transverse electrostatic bias of the filaments, the relative time delay of the orthogonal THz components can be modulated (Ⅰ), leading to the conversion of the output THz polarization states (Ⅱ)[66-68]

5.2 低泵浦功率下强太赫兹电场与增强

太赫兹波被约束在光丝中一个直径仅为微米量级的空间内，这意味着光丝中的太赫兹电场极强[56]，这是一种在低泵浦激光功率下获得强太赫兹电场的新方式。图 4（b-I）中的黑色实线显示太赫兹脉冲能量 ε_{THz} 随光丝传输距离 z 增加而增大，并最终在光丝末端（z=6 mm 之后）趋于饱和。图 4（b-I）中的圆点表示相应电场 E_{THz} 的变化，可以看出在光丝区域内（z<6 mm）太赫兹波展现出极强的电场强度，整体数值高于 520 kV/cm，最大可达 1.3 MV/cm，此时泵浦激光能量仅约为 0.5 mJ/pulse。以上现象可归因于太赫兹波在光丝区域的空间强束缚效应，极小的模场直径带来了极大的电场强度。对比之下，在光丝后端及远场（z>6 mm），太赫兹光束直径快速增大，故其电场强度随之减小。若进一步优化 BFD（倍频晶体到光丝焦点的距离），还可获得高达 1.58 MV/cm 的强太赫兹电场

振幅，如图 4(b-II)所示。但需要注意的是，以上小功率、大电场太赫兹源还应进一步在与物质的非线性相互作用中(如掺杂硅片对太赫兹波的非线性吸收[9])进行检验，这方面的实验工作本课题组正在开展。

另外，可以将光丝作为亚波长尺度的太赫兹点源进行密集排布形成阵列[69-72]，从而实现远场太赫兹辐射的相干增强。如：在泵浦激光光束中插入一片阶跃型相位板来产生平行双丝，则辐射的太赫兹电场振幅与单丝相比有 2 倍的增强[65]，见图 4(b-III)。在此基础上更换相位板产生光丝数量更多的太赫兹源阵列，可以实现更大倍率的辐射增强，而且信号强度与光丝数目成正比[73]。这种基于太赫兹“微源”叠加的电场增强方案可以打破单纯依靠提高泵浦功率导致的太赫兹输出饱和效应，从而更充分地利用泵浦激光能量实现更强太赫兹输出，而且不需要在光丝附近增加其他调控手段(如施加横向高压静电场等等[74-75])。特别地，该电场增强方案可以满足太赫兹电场的远程增强需求。

5.3 宽带太赫兹脉冲偏振态的灵活调控

太赫兹波被限制在光丝等离子体中传输，因此产生的太赫兹双折射效应会受到泵浦激光能量、等离子体密度和光丝长度等多个因素的影响，据此可以调节太赫兹脉冲两个正交分量之间的相对时间延迟，实现偏振调控的目的。比如，通过截取不同长度的单色场光丝可以实现太赫兹横波辐射的椭圆偏振到线偏振的转化[66]。再如，通过对单色光丝施加横向静电场并改变入射激光功率可以显著改变太赫兹正交分量的相对延迟[67,76][如图 4(c-I)所示]，进而使得太赫兹偏振态能够在线偏振、椭圆偏振、圆偏振之间灵活调控和转换[如图 4(c-II)所示]。

6 总结与展望

太赫兹波空间强束缚效应是飞秒激光成丝过程中一种新颖的实验现象，伴随着亚波长直径太赫兹光束传输与相速度超光速等典型特征，其探测过程催生出了突破等离子体烧蚀限制的近场光学诊断新技术，其机理可由结合了经典电磁理论和表面波原理的一维负介电常数波导(1DND)模型进行解释。太赫兹波空间强束缚效应促成了多个新颖应用并解决了本领域内的相关瓶颈难题，如能量无损超分辨率太赫兹成像、高转换效率太赫兹强电场的实现与增强以及宽带太赫兹脉冲偏振态灵活调控与转换等。太赫兹波空间强束缚效应作为飞秒激光成丝辐射太赫兹波的第三过程，已成为补全太赫兹波产生与传输图像的一块重要拼图，是架通宏观、微观经典理论(四波混频与瞬态光电流模型)的桥梁，据此提出的三过程模型成功解决了太赫兹波偏振矢量演变等问题，为重新审视本领域过去所积累的实验结论并化解相关矛盾提供了全新契机。

对太赫兹波空间强束缚效应的未来展望可以集中在如下几个方面：1)对于单、双色场成丝辐射太赫兹波的物理机制研究来说，由于太赫兹波空间强束缚效应的普适性，可尝试将其同时融入两个领域的太赫兹波产生过程中，为统一理解这两个重要研究方向的共性机理奠定基础；2)在新技术层面，太赫兹波被压缩到低数量级空间尺度内必将引领新的应用技术革新，如依赖于亚波长窄通道空间压缩的宽带太赫兹全光计算技术[77]，就有望在激光光丝平台上利用太赫兹波强束缚导引传输实现突破[78]；3)从跨学科角度看，可尝试将 1DND 模型与微纳光学相关原理进行交叉融合，借助表面波、ENZ(epsilon near zero)等概念，探索跨尺度的太赫兹波空间强束缚新理论，以表面等离子体激元波导这一新形态重新理解激光等离子体光丝[79]；4)基于太赫兹波空间强束缚效应，激光光丝将成为新的自平衡物理体系，其与太赫兹波的关系类似于硅基光纤波导与光的关系，此光丝平台将极大地促进人们在新视角下观察并研究新的激光电离机制、太赫兹波传输原理与调控方法。

参 考 文 献

[1] Tonouchi M. Cutting-edge terahertz technology[J]. Nature Photonics, 2007, 1(2): 97-105.

[2] 许景周, 张希成. 太赫兹科学技术和应用[M]. 北京: 北京大学出版社, 2007: 8.
Xu J Z, Zhang X C. Terahertz science and technology and its application[M]. Beijing: Peking University Press, 2007: 8.

[3] Redo-Sanchez A, Zhang X C. Terahertz science and technology trends[J]. IEEE Journal of Selected Topics in Quantum Electronics, 2008, 14(2): 260-269.

[4] Dhillon S S, Vitiello M S, Linfield E H, et al. The 2017 terahertz science and technology roadmap[J]. Journal of Physics D: Applied Physics, 2017, 50(4): 043001.

[5] Fülöp J A, Tzortzakis S, Kampfrath T. Laser-driven strong-field terahertz sources[J]. Advanced Optical Materials, 2020, 8(3): 1900681.

[6] Bergé L, Kaltenecker K, Engelbrecht S, et al. Terahertz spectroscopy from air plasmas created by two-color femtosecond laser pulses: the ALTESSE project[J]. EPL (Europhysics Letters), 2019, 126(2): 24001.

[7] Khalatpour A, Paulsen A K, Deimert C, et al. High-power portable terahertz laser systems[J]. Nature Photonics, 2021, 15(1): 16-20.

[8] Ropagnol X, Kovács Z, Gilicze B, et al. Intense sub-terahertz radiation from wide-bandgap semiconductor based large-aperture photoconductive antennas pumped by UV lasers[J]. New Journal of Physics, 2019, 21(11): 113042.

[9] Zhang B L, Ma Z Z, Ma J L, et al. 1.4-mJ high energy terahertz radiation from lithium niobates[J]. Laser & Photonics Reviews, 2021, 15(3): 2000295.

[10] Jolly S W, Matlis N H, Ahr F, et al. Spectral phase control of interfering chirped pulses for high-energy narrowband terahertz generation[J]. Nature Communications, 2019, 10: 2591.

[11] Liao G Q, Li Y T, Liu H, et al. Multi-millijoule coherent terahertz bursts from picosecond laser-irradiated metal foils[J]. Proceedings of the National Academy of Sciences of the United States of America, 2019, 116(10): 3994-3999.

[12] Zhang Z L, Chen Y P, Chen M, et al. Controllable terahertz radiation from a linear-dipole array formed by a two-color laser filament in air[J]. Physical Review Letters, 2016, 117(24): 243901.

[13] Zhang Z L, Chen Y P, Cui S, et al. Manipulation of polarizations for broadband terahertz waves emitted from laser plasma filaments

[J]. Nature Photonics, 2018, 12(9): 554-559.
[14] Zhang L L, Wang W M, Wu T, et al. Observation of terahertz radiation via the two-color laser scheme with uncommon frequency ratios[J]. Physical Review Letters, 2017, 119(23): 235001.
[15] Zhao H, Tan Y, Zhang L L, et al. Ultrafast hydrogen bond dynamics of liquid water revealed by terahertz-induced transient birefringence[J]. Light: Science & Applications, 2020, 9: 136.
[16] Zhang L L, Wang W M, Wu T, et al. Strong terahertz radiation from a liquid-water line[J]. Physical Review Applied, 2019, 12(1): 014005.
[17] Koulouklidis A D, Gollner C, Shumakova V, et al. Observation of extremely efficient terahertz generation from mid-infrared two-color laser filaments[J]. Nature Communications, 2020, 11: 292.
[18] Dey I, Jana K, Fedorov V Y, et al. Highly efficient broadband terahertz generation from ultrashort laser filamentation in liquids[J]. Nature Communications, 2017, 8: 1184.
[19] Balakin A V, Coutaz J L, Makarov V A, et al. Terahertz wave generation from liquid nitrogen[J]. Photonics Research, 2019, 7(6): 678-686.
[20] Zhao J Y, Wang Q N, Hui Y C, et al. Traveling-wave antenna model for terahertz radiation from laser-plasma interactions[J]. SciPost Physics Core, 2022, 5(3): 46.
[21] Yu Z Q, Sun L, Zhang N, et al. Anti-correlated plasma and THz pulse generation during two-color laser filamentation in air[J]. Ultrafast Science, 2022, 2022: 9853053.
[22] 戴建明, 张祎帆, 陈宇轩, 等. 液态水辐射源产生太赫兹波的研究进展[J]. 中国激光, 2021, 48(19): 1914001.
Dai J M, Zhang Y F, Chen Y X, et al. Research progress on terahertz wave generation from liquid water[J]. Chinese Journal of Lasers, 2021, 48(19): 1914001.
[23] 惠雨晨, 赵佳宇. 外电场作用下飞秒激光成丝辐射太赫兹波的全电流模型[J]. 光学学报, 2022, 42(1): 0114002.
Hui Y C, Zhao J Y. Full current model for terahertz wave generation from femtosecond laser filament under external electric fields[J]. Acta Optica Sinica, 2022, 42(1): 0114002.
[24] Roskos H G, Thomson M D, Kreß M, et al. Broadband THz emission from gas plasmas induced by femtosecond optical pulses: from fundamentals to applications[J]. Laser & Photonics Reviews, 2007, 1(4): 349-368.
[25] Clerici M, Peccianti M, Schmidt B E, et al. Wavelength scaling of terahertz generation by gas ionization[J]. Physical Review Letters, 2013, 110(25): 253901.
[26] Oh T I, Yoo Y J, You Y S, et al. Generation of strong terahertz fields exceeding 8 MV/cm at 1 kHz and real-time beam profiling [J]. Applied Physics Letters, 2014, 105(4): 041103.
[27] Wang T J, Yuan S A, Chen Y P, et al. Toward remote high energy terahertz generation[J]. Applied Physics Letters, 2010, 97(11): 111108.
[28] Liu J L, Dai J M, Chin S L, et al. Broadband terahertz wave remote sensing using coherent manipulation of fluorescence from asymmetrically ionized gases[J]. Nature Photonics, 2010, 4(9): 627-631.
[29] Hamster H, Sullivan A, Gordon S, et al. Subpicosecond, electromagnetic pulses from intense laser-plasma interaction[J]. Physical Review Letters, 1993, 71(17): 2725-2728.
[30] D'Amico C, Houard A, Franco M, et al. Conical forward THz emission from femtosecond-laser-beam filamentation in air[J]. Physical Review Letters, 2007, 98(23): 235002.
[31] Amico C D, Houard A, Akturk S, et al. Forward THz radiation emission by femtosecond filamentation in gases: theory and experiment[J]. New Journal of Physics, 2008, 10(1): 013015.
[32] Cook D J, Hochstrasser R M. Intense terahertz pulses by four-wave rectification in air[J]. Optics Letters, 2000, 25(16): 1210-1212.
[33] Kim K Y, Glownia J H, Taylor A J, et al. Terahertz emission from ultrafast ionizing air in symmetry-broken laser fields[J]. Optics Express, 2007, 15(8): 4577-4584.
[34] Kim K Y, Taylor A J, Glownia J H, et al. Coherent control of terahertz supercontinuum generation in ultrafast laser-gas interactions[J]. Nature Photonics, 2008, 2(10): 605-609.
[35] Andreeva V A, Kosareva O G, Panov N A, et al. Ultrabroad terahertz spectrum generation from an air-based filament plasma[J]. Physical Review Letters, 2016, 116(6): 063902.
[36] Zhao J Y, Liu W W, Li S C, et al. Clue to a thorough understanding of terahertz pulse generation by femtosecond laser filamentation[J]. Photonics Research, 2018, 6(4): 296.
[37] de Alaiza Martínez P G, Babushkin I, Bergé L, et al. Boosting terahertz generation in laser-field ionized gases using a sawtooth wave shape[J]. Physical Review Letters, 2015, 114(18): 183901.
[38] Karpowicz N, Zhang X C. Coherent terahertz echo of tunnel ionization in gases[J]. Physical Review Letters, 2009, 102(9): 093001.
[39] You Y S, Oh T I, Kim K Y. Off-axis phase-matched terahertz emission from two-color laser-induced plasma filaments[J]. Physical Review Letters, 2012, 109(18): 183902.
[40] Johnson L A, Palastro J P, Antonsen T M, et al. THz generation by optical Cherenkov emission from ionizing two-color laser pulses [J]. Physical Review A, 2013, 88(6): 063804.
[41] Dietze D, Darmo J, Roither S, et al. Polarization of terahertz radiation from laser generated plasma filaments[J]. Journal of the Optical Society of America B, 2009, 26(11): 2016-2027.
[42] Chen Y P, Marceau C, Génier S, et al. Elliptically polarized terahertz emission through four-wave mixing in a two-color filament in air[J]. Optics Communications, 2009, 282(21): 4283-4287.
[43] You Y S, Oh T I, Kim K Y. Mechanism of elliptically polarized terahertz generation in two-color laser filamentation[J]. Optics Letters, 2013, 38(7): 1034-1036.
[44] Zhang Y Z, Chen Y P, Xu S Q, et al. Portraying polarization state of terahertz pulse generated by a two-color laser field in air[J]. Optics Letters, 2009, 34(18): 2841-2843.
[45] Zhao J Y, Zhang Y Z, Zeng T, et al. Correlated study of terahertz pulse generation and plasma density during two-color filamentation in air[C]//CLEO: Applications and Technology 2015, May 10-15, 2015, San Jose, California. Washington, D.C.: Optica Publishing Group, 2015: JTu5A.9.
[46] Xu S Q, Zhang Y Z, Zheng Y B, et al. Study of physical mechanism of two-color laser field pumped THz wave in air plasma [J]. Terahertz Science and Technology, 2010, 3(3): 130.
[47] Zhang Y Z, Chen Y Y, Marceau C, et al. Non-radially polarized THz pulse emitted from femtosecond laser filament in air[J]. Optics Express, 2008, 16(20): 15483-15488.
[48] Chen Y P, Marceau C, Liu W W, et al. Elliptically polarized terahertz emission in the forward direction of a femtosecond laser filament in air[J]. Applied Physics Letters, 2008, 93(23): 231116.
[49] Gorodetsky A, Koulouklidis A D, Massaouti M, et al. Physics of the conical broadband terahertz emission from two-color laser-induced plasma filaments[J]. Physical Review A, 2014, 89(3): 033838.
[50] Blank V, Thomson M D, Roskos H G. Spatio-spectral characteristics of ultra-broadband THz emission from two-colour photoexcited gas plasmas and their impact for nonlinear spectroscopy[J]. New Journal of Physics, 2013, 15(7): 075023.
[51] Klarskov P, Strikwerda A C, Iwaszczuk K, et al. Experimental three-dimensional beam profiling and modeling of a terahertz beam generated from a two-color air plasma[J]. New Journal of Physics, 2013, 15(7): 075012.
[52] Zhong H A, Karpowicz N, Zhang X C. Terahertz emission profile from laser-induced air plasma[J]. Applied Physics Letters, 2006, 88(26): 261103.
[53] Klarskov P, Zalkovskij M, Strikwerda A C, et al. Spectrally resolved measurements of the terahertz beam profile generated from a two-color air plasma[C]//2014 Conference on Lasers and Electro-Optics (CLEO)-Laser Science to Photonic Applications,

June 8-13, 2014, San Jose, CA, USA. New York: IEEE Press, 2014.
[54] Chin S L, Wang T J, Marceau C, et al. Advances in intense femtosecond laser filamentation in air[J]. Laser Physics, 2012, 22(1): 1-53.
[55] Couairon A, Mysyrowicz A. Femtosecond filamentation in transparent media[J]. Physics Reports, 2007, 441(2/3/4): 47-189.
[56] Zhao J Y, Chu W, Wang Z, et al. Strong spatial confinement of terahertz wave inside femtosecond laser filament[J]. ACS Photonics, 2016, 3(12): 2338-2343.
[57] Liu C, Chen Y M, Zhao J Y, et al. Plasma micro-cavity of terahertz wave during laser filamentation[J]. IEEE Photonics Journal, 2019, 11(4): 5900714.
[58] Zhao J Y, Zhang X, Li S, et al. Detecting the propagation effect of terahertz wave inside the two-color femtosecond laser filament in the air[J]. Applied Physics B, 2018, 124(3): 45.
[59] Zhao J Y, Zhang Y Z, Wang Z, et al. Propagation of terahertz wave inside femtosecond laser filament in air[J]. Laser Physics Letters, 2014, 11(9): 095302.
[60] 刘伟伟, 赵佳宇, 张逸竹, 等. 飞秒激光成丝过程中的太赫兹波超光速传输现象研究[J]. 红外与激光工程, 2016, 45(4): 15-21.
Liu W W, Zhao J Y, Zhang Y Z, et al. Research on superluminal propagation of terahertz wave during femtosecond laser filamentation[J]. Infrared and Laser Engineering, 2016, 45(4): 15-21.
[61] Zhao J Y, Chu W, Guo L J, et al. Terahertz imaging with sub-wavelength resolution by femtosecond laser filament in air[J]. Scientific Reports, 2014, 4: 3880.
[62] Takahara J, Yamagishi S, Taki H, et al. Guiding of a one-dimensional optical beam with nanometer diameter[J]. Optics Letters, 1997, 22(7): 475-477.
[63] Lu D, Gao H, Zhao J Y, et al. Numerical simulation on terahertz wave propagation in plasma channels[J]. Optik, 2019, 182: 42-49.
[64] Bozhevolnyi S I. Plasmonic nanoguides and circuits[M]. Singapore: Pan Stanford Publishing, 2008.
[65] Zhao J Y, Guo L J, Chu W, et al. Simple method to enhance terahertz radiation from femtosecond laser filament array with a step phase plate[J]. Optics Letters, 2015, 40(16): 3838-3841.
[66] Zhao J Y, Gao H, Li S C, et al. Investigating the non-radially polarized component of terahertz wave emission during single-colour femtosecond laser filamentation in air[J]. Journal of Optics, 2018, 20(10): 105502.
[67] Yu Z Q, Su Q, Zhang N, et al. THz birefringence inside femtosecond laser filament in air[J]. Optics & Laser Technology, 2021, 141: 107179.
[68] Zhao J Y, Liu W W. Two-dimensional terahertz time-domain spectroscopy and its applications[J]. Journal of Electronic Science and Technology, 2015, 13(1): 6-13.
[69] Tang L Z, Zhao J Y, Dong Z H, et al. Towards remotely directional transmission of terahertz wave in air: the concept of free-space photonic crystal waveguide[J]. Optics & Laser Technology, 2021, 141: 107102.
[70] Gao H, Chu W, Yu G L, et al. Femtosecond laser filament array generated with step phase plate in air[J]. Optics Express, 2013, 21(4): 4612-4622.
[71] Panov N A, Kosareva O G, Murtazin I N. Ordered filaments of a femtosecond pulse in the volume of a transparent medium[J]. Journal of Optical Technology, 2006, 73(11): 778-785.
[72] 高慧, 赵佳宇, 刘伟伟. 超快激光成丝现象的多丝控制[J]. 光学精密工程, 2013, 21(3): 598-607.
Gao H, Zhao J Y, Liu W W. Control of multiple filamentation induced by ultrafast laser pulses[J]. Optics and Precision Engineering, 2013, 21(3): 598-607.
[73] 鲁丹, 苏强, 齐鹏飞, 等. 基于光丝阵列的太赫兹辐射增强方法[J]. 中国激光, 2019, 46(6): 0614021.
Lu D, Su Q, Qi P F, et al. Method for terahertz radiation enhancement using filament array[J]. Chinese Journal of Lasers, 2019, 46(6): 0614021.
[74] Shipilo D E, Nikolaeva I A, Pushkarev D V, et al. Balance of emission from THz sources in DC-biased and unbiased filaments in air[J]. Optics Express, 2021, 29(25): 40687-40698.
[75] Nikolaeva I A, Shipilo D E, Pushkarev D V, et al. Flat-top THz directional diagram of a DC-biased filament[J]. Optics Letters, 2021, 46(21): 5497-5500.
[76] Su Q A, Xu Q A, Zhang N, et al. Control of terahertz pulse polarization by two crossing DC fields during femtosecond laser filamentation in air[J]. Journal of the Optical Society of America B, 2019, 36(10): G1-G5.
[77] Balistreri G, Tomasino A, Dong J L, et al. Time-domain integration of broadband terahertz pulses in a tapered two-wire waveguide[J]. Laser & Photonics Reviews, 2021, 15(8): 2100051.
[78] Zhao J Y. Air-plasma-based all-optical temporal integration of broadband terahertz pulses[EB/OL]. (2022-11-13) [2023-02-04]. https://arxiv.org/abs/2211.06804.
[79] Zhao J Y. Observation of the epsilon-near-zero (ENZ) effect inside the laser plasma in air[EB/OL]. (2022-11-13)[2023-02-04]. https://arxiv.org/abs/2211.06796.

Strong Spatial Confinement of Terahertz Waves Along Laser Plasma Filaments

Zhao Jiayu[1], Han Yongpeng[1], Zhu Feifan[1], Guo Lanjun[2], Zhang Yizhu[3], Peng Yan[1], Zhu Yiming[1], Liu Weiwei[2*]

[1]*Terahertz Technology Innovation Research Institute, University of Shanghai for Science and Technology, Shanghai* 200093, *China*;

[2]*Institute of Modern Optics, Nankai University, Tianjin* 300350, *China*;

[3]*School of Precision Instrument and Opto-Electronics Engineering, Tianjin University, Tianjin* 300072, *China*

Abstract

Significance Femtosecond laser filamentation in air refers to the technical approach of using the femtosecond laser to ionize air near its focal point, forming a plasma channel (also known as the optical filament) that emits terahertz (THz) waves. Due to the remote generation of plasma filaments and the broadband and high intensity characteristics of the emitted THz waves, femtosecond laser filamentation overcomes water vapor absorption losses in free-space THz transmission; thus, it is advantageous for applications such as remote sensing and communication in THz band. Therefore, the study of physical mechanisms of THz wave radiation by

femtosecond laser filaments has become an important branch of THz science.

However, there currently remains controversy surrounding the mainstream models for THz wave generation, and important experimental observations such as THz polarization and angular dispersion distribution remain in disagreement. For example, the two mainstream models, i.e., four-wave mixing (4WM) and photocurrent (PC), have fundamental differences: when the THz wave yield is significant, the former assumes a relative phase difference of 0 between the fundamental and second harmonic laser fields, while the latter assumes a $\pi/2$ phase difference. Furthermore, regarding the dependence of the far-field divergence angle of THz waves on frequency, the mainstream viewpoint represented by the off-axis phase matching model suggests that only dual-color filaments longer than the dephasing length can radiate THz waves with high-frequency components distributed inside and low-frequency components distributed outside. However, this explanation fails to account for the similar radiation behavior observed in short filaments, and contradicts experimental findings in some literature, which report high-frequency outside, low-frequency inside, or frequency-independent angular distribution.

Progress These unresolved contradictions pose significant challenges in the study of THz wave radiation from dual-color filaments. The reason for these contradictions could be that femtosecond laser filamentation is a complex optical phenomenon involving multiple nonlinear processes such as optical Kerr self-focusing and plasma defocusing. Therefore, a single physical model is likely insufficient to encompass the entire dynamic mechanism of filamentation-induced THz wave radiation. Accordingly, we propose a three-process theory that incorporates mainstream models and the recent experimental observation of spatial confinement of THz waves inside the laser filament.

We first divided the filamentation process into Kerr self-focusing and plasma defocusing before and after the laser intensity breaking the ionization threshold. Then, in the first process, when neutral gas molecules are not yet ionized, we primarily consider the 4WM effect of the pump laser and its harmonic in air, which generates THz waves. The second process occurs when the laser intensity exceeds the ionization threshold, resulting in the ionization of air and the formation of a plasma (free electrons). Under the drive of the time-asymmetric electric field of the dual-color laser pulse, the plasma oscillates and gives rise to a nonzero trailing current (also known as drift current or residual current) and the emission of THz waves. Finally, considering the time scale of THz waves (ps), which is much larger than the establishment time of the plasma filament (tens or hundreds of fs) and much smaller than the plasma lifetime (ns), the filament can be treated as a quasistatic waveguide for THz waves. During the transmission of THz wave, its interaction with the plasma free electrons leads to the spatial confinement of THz waves at the radial edge of the filament. This constitutes the third process.

Based on the analysis above, we explain the THz radiation regarding the three processes using the mainstream models of 4WM and PC, as well as the proposed one-dimensional negative dielectric waveguide model (1DND). As shown in Fig. 1, if we consider only the first or second process, the predictions of the THz orthogonal polarization components by the two mainstream models alone are unsatisfactory. If we incorporate the THz spatial confinement effect as the crucial third process, it is necessary to consider the spatial mode distribution, energy loss, and spectral changes of THz waves after interaction with the plasma. This consideration leads to the best fit to experimental results. The THz spatial confinement effect has also facilitated several novel applications and addressed key challenges in the field (Fig. 4), including super-resolution THz imaging, high conversion efficiency of THz strong electric fields, and flexible manipulation of broadband THz polarization states.

Conclusions and Prospects In conclusion, the proposed 4WM+PC+1DND model presents a new mechanism that overcomes the limitations of a single physical model, bridges the connections between mainstream models, and provides a unified framework for fundamental theories that were previously incompatible. This model could comprehensively and reasonably explain the unresolved evolution of THz polarization states with the rotation of the frequency-doubling crystal in dual-color field radiation, as well as experimental results such as near-field THz modes and far-field THz spatial chirping. It provides a fresh opportunity to reevaluate past experimental findings and resolve related contradictions in the field.

Future prospects of the THz spatial confinement effect can be focused on the following aspects. 1) Investigation of the physical mechanisms behind single-color and dual-color filamentation for THz wave generation: due to the universality of the THz spatial confinement effect, it can be incorporated into both single-color and dual-color THz generation processes. This might establish a foundation for a unified understanding of the common mechanisms in these two important research directions. 2) Exploration of new technologies: compressing THz waves into subwavelength spatial scales is expected to lead to technological innovations. For example, broadband THz all-optical computation techniques relying on spatial compression in subwavelength narrow channels can be developed utilizing THz wave spatial confinement for guidance and transmission, which has the potential for breakthroughs in this field. 3) Interdisciplinary exploration: the integration of the 1DND model with principles from micro and nanooptics can be explored. Concepts such as surface waves and epsilon near zero (ENZ) can be utilized to investigate THz spatial confinement across scales ranging from submillimeter to nanometer. This approach can provide new insights into laser-induced plasma filaments using the concept of surface plasmon polariton waveguides. 4) Laser filaments as self-balanced physical systems: based on the THz spatial confinement effect, laser filaments in the THz regime can become a new platform for self-balanced physical systems. Similar to the action of silicon-based fiber waveguides on light, this filament platform can greatly facilitate the study of new laser ionization mechanisms, THz wave transmission principles, and modulation methods from a new perspective.

Key words physical optics; terahertz wave; femtosecond laser filamentation; spatial confinement; physical mechanism; super-resolution imaging